Structure and Matrix Isolation Infrared Spectrum of Formyl Fluoride Dimer: Blue-Shift of the C−H Stretching Frequency

Jussi M. E. Ahokas, Kari J. Vaskonen, and Henrik M. Kunttu*

Nanoscience Center, Department of Chemistry, P.O. Box 35, 40014 University of Jyväskylä, Finland

Received: February 24, 2006; In Final Form: April 27, 2006

Infrared spectroscopy (IR) of formyl fluoride (HCOF) dimer is studied in low-temperature argon and krypton matrixes. New IR absorptions, ca. 17 cm^{-1} blue shifted from the monomer C−H stretching fundamental, are assigned to the HCOF dimer. The MP2/6-311++G** calculations were utilized to define structures and harmonic frequencies of various HCOF dimers. Among the four optimized structures, the dimer having two C−H···O hydrogen bonds possesses strongest intermolecular bonding. The calculated harmonic frequencies of this dimer structure are shifted from the monomer similarly as observed in the experiment. Thus, we suggest that the experimentally observed blue shifted C−H bands belong to the dimer with two C−H···O hydrogen bonds. This observation includes the HCOF dimer to the class of hydrogen bonded complexes showing blue shift in their vibrational energies.

Introduction

Hydrogen bonding (H-bonding) is common and one of the strongest intermolecular interactions keeping molecules together. The great importance of H-bonding in chemistry, physics, and biology, that is, its importance for life, has fascinated scientists since the beginning of the 20th century.[1]

The characteristic structure of H-bond is of the X−H···Y type, where X and Y are electronegative elements, typically O, N, halogens, or a region of excess electron density like aromatic π-systems and Y possesses one or two lone electron pairs.[1] In addition to highly electronegative elements, the H-bond, although weaker, appears between the C−H hydrogen and Y. The origin of the H-bonding is explained as arising dominantly from electrostatic interaction, while charge-transfer effects are of secondary importance.[2] The charge transfer from the proton acceptor (Y) to the proton donor (X−H), which increases electron density in the antibonding orbital of the X−H proton donor is characteristic of the hydrogen bond. This, in turn, leads to weakening of the X−H bond. Weakening and concomitant elongation of the bond are typically observed as a red shift in the X−H stretching frequency compared to the free donor. This behavior was considered as an exclusive property of the H-bond until in the 1980s the first evidence of the opposite case was reported. It was shown that, in fact, the formation of the C−H···Y H-bond in triformylmethane was accompanied by a blue shift in the C−H stretching frequency.[3] It was suggested by Hobza and Havlas[4] that such unexpected behavior may be ascribed to a charge transfer from the proton acceptor to a remote region of the H-bonded complex instead of increasing electron density of the antibonding X−H orbital. This would lead to structural reorganization and shortening of the X−H bond and blue shift of the X−H stretching frequency of the complex. However, the origin of the blue shift is not fully understood, and recent experimental and theoretical studies are reviewed in refs 5−7.

Most relevant to the present study is the recent article by Kovács et al. in which the authors report blue shift of the C−H stretching frequency in quantum chemical calculations of HCOY (Y = H, CH_3, F, Cl, Br, I) dimers at the MP2/6-311++G** level of theory.[8] The optimized structures showed lengthening of the contacting C−X (X = O, halogens) bonds and shortening of the C−H bonds. Consistently, the natural bond orbital analysis showed slight decrease in the population of the antibonding orbital of the C−H bond.

In this article we present experimental observations of blue shift of the C−H stretching frequency in infrared spectrum of HCOF dimer in cryogenic argon and krypton matrixes. To support the spectral assignments, we carried out quantum chemical calculations for geometry optimization and harmonic frequencies of HCOF monomer and dimer structures. We have recently reported the photochemistry of the HCOF monomer in rare gas matrix hosts.[9]

Experimental Details

Formyl fluoride was prepared from formic acid (Riedel-de Haën), benzoyl chloride (Merck), and potassium hydrogen fluoride (Aldrich) according to a method by Olah and Kuhn[10] and purified by a low-temperature distillation. The pure formyl fluoride was stored in a Pyrex container and kept under liquid nitrogen.

Formyl fluoride was mixed in a vacuum line with argon (Aga, 99.9999%) or krypton (Aga, 99.997%) prior to matrix isolation experiments. The gas mixtures were deposited onto a low-temperature CsI substrate attached to the coldfinger of a closed-cycle helium cryostat (APD Cryogenics, DE-202A). The deposition rate was typically ca. 0.04 mmol/min and the total amount of deposited gas was 2−4 mmol. The temperature of the substrate was held at 10−35 K during the deposition, and all spectral measurements were carried out at 10 K. The cryostat was equipped with CsI windows for infrared measurements.

Infrared spectra were recorded with a Nicolet Magna IR 760 spectrometer equipped with a HgCdTe detector and a KBr beam splitter. The spectral resolution was 0.125−0.5 cm^{-1}.

* To whom correspondence should be addressed. E-mail: hekunttu@jyu.fi.

10.1021/jp061188x CCC: $33.50
Published on Web 06/08/2006

Computational Details

The calculations with all electrons correlated were carried out using second-order Møller−Plesset perturbation theory[11] with the Gaussian 03 program package.[12] The geometry optimization and the frequency calculations of the monomer and the dimers were carried out using the 6-311++G** basis set for all atoms.[13] The geometry optimization was carried out with the keyword VeryTight in the Gaussian 03 software, meaning that the criterion for convergence of the RMS force was set to 1×10^{-6} au. This is necessary for systems possessing low-frequency vibrations in order to find their lowest energy structures and hence the proper harmonic frequencies. The basis set superposition error (BSSE) was corrected according to the counterpoise (CP) method.[14] The CP method is implemented in the Gaussian 03 program, and correction was performed on every iteration step. The advantage of this procedure is that it includes BSSE correction in both the energy and the final structure. In addition, the BSSE corrected geometry contributes to the frequency calculation.

Experimental Results

After the deposition of formyl fluoride in an argon matrix (HCOF/Ar = 1/500) at 10 K, five of the six normal vibrations of HCOF monomer, two dimer absorptions at 1818.5 and 672 cm^{-1}, and the absorption of carbon monoxide were observed in the infrared spectrum.[9,15] The appearance of CO in the sample indicates decomposition of HCOF during the deposition. However, there was no evidence of HF in the IR spectrum. Additionally to CO absorption, only minor traces of water absorption was observed in the IR spectrum. The absorptions of the HCOF monomer and CO were accompanied by broad red-shifted shoulder bands with more or less resolved structure. Other absorptions were observed at 1712, 1031.9, and 1023.0 cm^{-1}.

A closer look at the spectrum shows that the vibrational bands of the HCOF monomer are split into two lines. Gradual annealing of the sample sharpened and slightly decreased the intensities of the absorption lines of the monomer, and after annealing at 30 K, the monomer absorptions consisted of two clearly separated lines as presented in our previous study.[9] It is also worth mentioning that the single absorption line at 1023.0 cm^{-1} sharpened as well. Simultaneously, the broad shoulder bands of the HCOF absorptions were gradually bleached, and the dimer bands at 1818 and 672.7 cm^{-1} gradually gained intensity upon annealing. After annealing, the dimer band at 1818 cm^{-1} was separated into two maxima at 1818.6 and 1818.0 cm^{-1}. The intensity of the carbon monoxide absorption decreased upon annealing, as well. Figure 1 illustrates the effect of annealing in the CO stretching region.

Upon annealing, new lines appeared at 2146.3, 2144.9, 2117.2, 2116.3, 1824.9, 1822.8, 1821.5, 1816.7, 1814.5, 1811.8, 1054.2 (shoulder band), 1052.7, 1051.7, 1049.4, 1048.4, and 1045.7 cm^{-1}. In addition, weak and broad absorption features with more or less resolved peaks appeared on the red side of the CO and CF stretching vibrations of the HCOF monomer.

Deposition of the samples at 15 K favored formation of HCOF dimers and increased the dimer-to-monomer ratio by a factor of 2. Moreover, the ratio between intensities of the red-shifted shoulder bands and the monomer bands decreased by a factor of ca. 3, and the ratio between CO and its red-shifted shoulder decreased by a factor of 3. The monomer bands showed two components, and the overall IR spectrum recorded after deposition showed similar spectral features as the sample deposited at 10 K and subsequently annealed at 20−25 K.

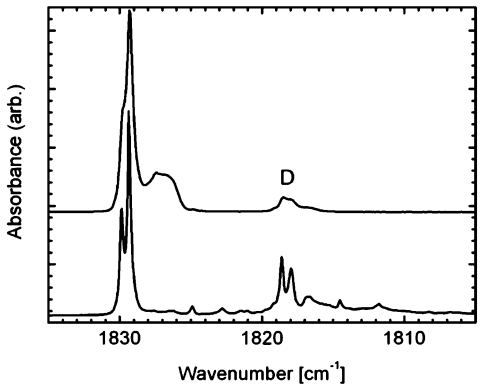

Figure 1. The IR absorption of the CO stretching mode of HCOF in argon matrix (HCOF/Ar = 1/500). Upper trace: after deposition at 10 K; lower trace: subsequent annealing at 30 K. Dimer band location is marked with D.

Annealing the matrix at 30 K induced similar spectral changes as described for the 10 K deposit.

A dramatic change in the IR spectrum was observed when the sample was deposited at 25 K. Individual monomer lines were split into two peaks as previously described, and the dimer bands gained intensity compared to the monomer bands. The broad red shifted shoulder bands of HCOF were absent, and several new absorption lines appeared nearby the monomer and dimer absorptions. Interestingly, a new line appeared on the blue side of the CH stretching absorption at 3013 cm^{-1} with weaker peaks on both sides of the main peak. The absorption of carbon monoxide at 2138.5 cm^{-1} was completely absent indicating some loss mechanism of the isolated carbon monoxide during the deposition. Annealing the sample at 35 K caused only minor changes to the spectrum. Figure 2 illustrates the effect of deposition temperature on the spectrum. Noteworthy, a reference experiment with HCOF/CO/Ar gas mixture showed significant increase or appearance of absorption bands at 3007, 3004, 3001, 2146.3, 2144.9, 2142.8, 1826.6, 1824.9, 1816.7, 1057.2, 1054.3, and 665 cm^{-1}.

To study spectral effects induced by the solid rare gas host we deposited a sample of HCOF in krypton (1:500) at 15 and 30 K. The spectral features of the 15 K krypton matrix were quite similar to the HCOF/Ar matrix (T_d = 10, 1:500) with spectral shifts in accordance with typical matrix experiments.[16] Furthermore, annealing the sample at 35 K caused similar changes in the spectrum as described for the annealed argon matrix. The IR spectrum of the krypton matrix deposited at 30 K showed the same, but shifted, spectral features as recorded from the argon matrix deposited at 25 K (Figure 3). Importantly, also in krypton a new absorption appeared to the higher energy side of the CH-stretching absorption.

The absorption at 1038.2 cm^{-1} in the argon matrix has been previously assigned to the out-of-plane vibration of a H atom from the plane of the HCOF molecule.[15] However, our experiments showed that this peak appears only after annealing the sample at 30 K and is more likely due to a thermally induced product.

Not only CO, but also water and HF may form complexes with HCOF. To provide more rigorous spectral analysis, the spectral observations related to water and HF must be taken into consideration. As mentioned above, there was no observation of HF in the course of this study. This might be because of reactions of HF on the walls of deposition system. Minor traces of water were observed in some experiments. Comparison of the spectrum where water was observed to the spectrum without water absorptions indicated that the known absorptions

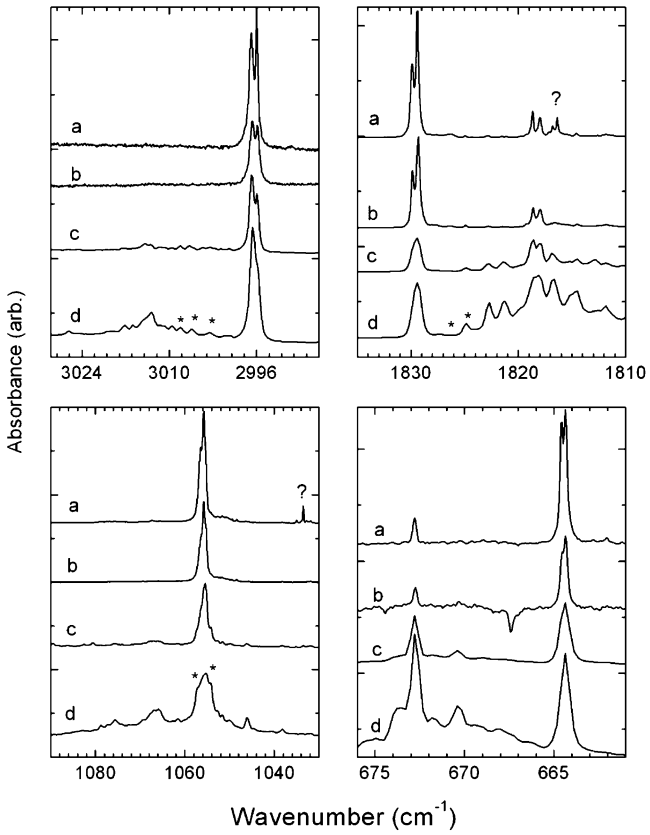

Figure 2. IR spectra of HCOF/Ar matrixes: (a) 1/2000, $T_d = 15$ K; (b) 1/500, $T_d = 15$ K; (c) 1/500, $T_d = 25$ K; (d) 1/250, $T_d = 25$ K. The positions of peaks that appear and/or gain intensity by carbon monoxide doping are indicated with an asterisk. Negative signals in the spectrum (b) in the right lower panel are due to spectral correction of the gas-phase CO_2. Note: The spectra c and d are recorded with resolution of 0.5 cm^{-1}.

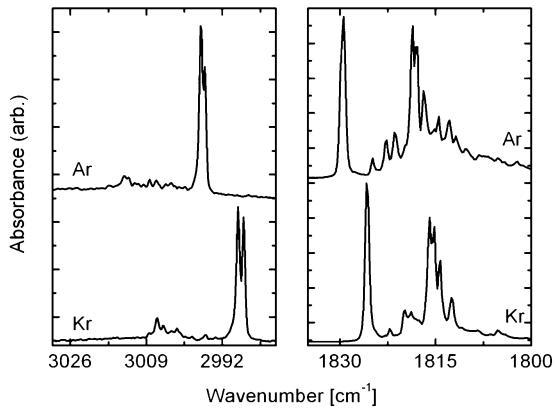

Figure 3. IR spectra of the CH and CO stretching regions of HCOF in argon (1/500, $T_d = 25$ K) and krypton (1/500, $T_d = 30$ K) matrixes.

of HCOF dimer as well as absorption at 3113 cm^{-1} were not affected by impurity water.

Computational Results

The optimized geometries of the HCOF monomer and four HCOF dimer structures are presented in Figure 4, and their structural parameters are collected in Table 1. Starting geometries for the monomer and the dimers were taken from literature.[8,17] We also tested other starting geometries for HCOF, which have been found stable for formaldehyde,[18] formic acid,[19] and acetaldehyde dimers.[20] According to previous study by Kovács et al., there are six stable HCOF dimer structures.[8] The

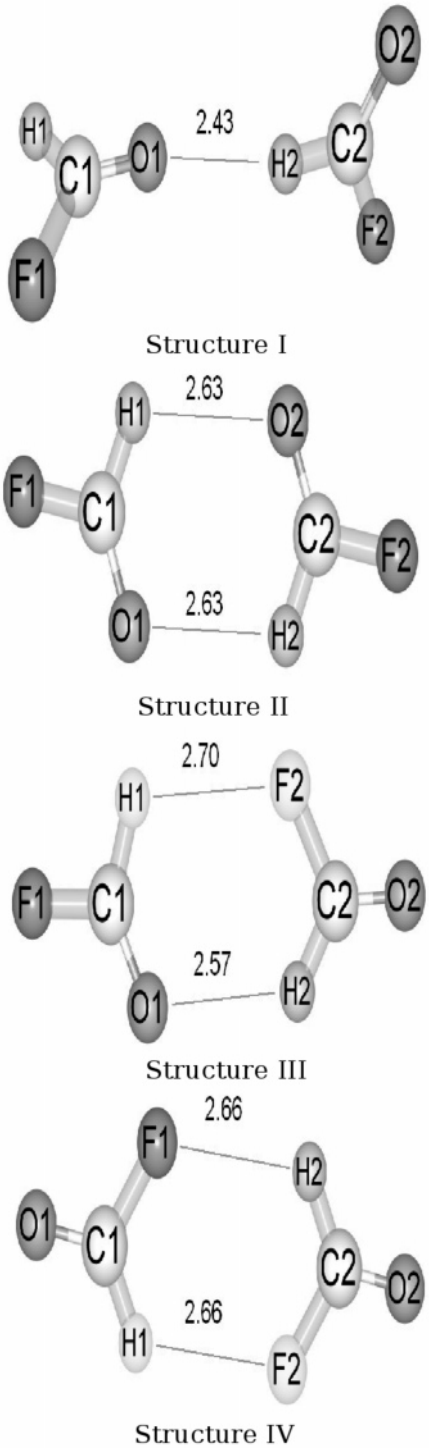

Figure 4. The optimized structures (MP2/6-311++G** with BSSE correction) of the HCOF dimer.

authors of ref 8 used the MP2/6-311++G** level of theory with the frozen core approximation in geometry optimization, and the BSSE was corrected for the final structures only. Moreover, the authors noted that the 6-311++G** basis set underestimates the dispersion interaction, while the BSSE does not fully compensate this error and the CP correction even increases the underestimation. Consequently, the authors of ref 8 concluded that the MP2/6-311++G** level, without the BSSE correction, yields better description of molecular properties compared to the BSSE corrected ones. In the present study we obtained six stable dimer structures similar to the ones reported in ref 8, when geometry optimization was carried out at the

TABLE 1: The MP2(FULL)/6-311++G (with BSSE Correction) Optimized Geometries of the HCOF Monomer and Four Stable Dimer Structures[a]**

	monomer	expt[b]	I	II	III	IV	V[c]	VI[d]
r_{C1H1}	1.093	1.095(8)	1.093	1.092	1.093	1.092		
r_{C1O1}	1.184	1.181(5)	1.186	1.187	1.187	1.183		
r_{C1F1}	1.350	1.338(5)	1.344	1.346	1.345	1.360		
a_{H1C1O1}	128.1	127.77(30)	127.8	127.7	127.8	129.0		
a_{H1C1F1}	109.0	109.90(300)	109.4	109.9	109.7	108.7		
r_{C2H2}			1.092	1.092	1.092	1.092		
r_{C2O2}			1.185	1.187	1.183	1.183		
r_{C2F2}			1.354	1.347	1.362	1.360		
a_{H2C2O2}			128.4	127.7	129.3	129.0		
a_{H2C2F2}			109.2	109.9	108.5	108.7		
r_{O1H2}			2.429	2.632	2.570		(3.108)	(2.608)
			(2.358)	(2.559)	(2.506)			
r_{H1O2}				2.632			(2.648)	
				(2.559)				
r_{H1F2}					2.704	2.665		(3.642)
					(2.571)	(2.551)		
r_{F1H2}						2.665		
						(2.551)		
$d_{F1C1C2F2}$			88.3	180.0				
$d_{F1C1C2O2}$					180.0			
$d_{O1C1C2O2}$						180.0		

[a] Bond lengths in Å and bond angles in deg. Data in parentheses correspond to BSSE uncorrected calculations. [b] Experimental data from ref 21. [c] Dimer with nearly perpendicular planes of monomers and double −H···O− hydrogen bond. See ref 8 for structure. [d] Dimer with −H···O- and −H···F− hydrogen bonds and nonplanar structure. See ref 8 for structure.

TABLE 2: Harmonic Frequencies (in cm^{-1}) at the MP2(FULL)/6-311++G Level[a]**

	monomer	I	II	III	IV
F1C1O1 bend	663.4 (22)	668.7 (16)			
F2C2O2 bend		661.1 (35)		655.9 (29)	
FCO bend in-phase			666.1 (0)	669.7 (19)	658.1 (0)
FCO bend out-of-phase			670.8 (39)		655.9 (57)
H1 OPLA[b]	1042.8 (0.002)	1047.4 (0.1)		1054.0 (0.0007)	
H2 OPLA[b]		1056.8 (1)		1052.1 (0.06)	
OPLA[b] in-phase			1058.3 (0.04)		1044.9 (0.06)
OPLA[b] out-of-phase			1059.3 (0)		1044.8 (0)
C1F1 str	1064.0 (297)	1082.8 (283)		1082.8 (303)	1020.5 (0)
C2F2 str		1049.9 (338)		1025.7 (318)	1043.3 (596)
CF str in-phase			1087.0 (0)		
CF str out-of-phase			1064.5 (692)		
H1 rock	1398.0 (0.4)	1399.6 (0.5)		1400.0 (0.4)	
H2 rock		1410.5 (0.3)		1392.5 (2.6)	
H rock in-phase			1393.0 (0)		1391.8 (0)
H rock in-phase			1398.2 (0.7)		1396.4 (1.4)
C1O1 str	1863.3 (268)	1860.3 (265)		1854.1 (384)	
C2O2 str		1855.7 (314)		1864.9 (2.6)	
CO str in-phase			1850.1 (0)		1870.2 (0)
CO str out-of-phase			1854.9 (530)		1861.4 (586)
C1H1 str	3172.3 (25)	3180.8 (22)		3185.4 (13)	
C2H2 str		3198.4 (0.9)		3197.1 (6)	
CH str. in-phase			3191.9 (0)		3191.8 (0)
CH str out-of-phase			3192.6 (19)		3191.1 (23)

[a] The computed IR intensities are given in parentheses. [b] Out of plane bend of C−H bond.

MP2/6-311++G** level with all electrons correlated and BSSE correction neglected. These geometries were then used as inputs for subsequent optimization including BSSE correction at every iteration step. Interestingly, two out of six structures that were found to be stable without BSSE correction, turned out to be unstable in the latter calculation. For example, the dimer with double C−H···O contacts and nearly perpendicular planes of monomers (structure VI in ref 8) relaxed to a structure with parallel planes of monomers (structure II in Figure 4). This demonstrates that use of basis sets not large enough to model the system properly may lead to a situation in which the choice of a method becomes crucial. For comparison, we present the BSSE corrected and the BSSE uncorrected data separately in the following tables.

Harmonic frequencies were calculated for the four stable dimer structures as well as for the monomer at the MP2(FULL)/6-311++G** level at optimized structures. The calculated frequencies are collected in Table 2. The relative energies of the dimer structures with respect to two separated HCOF molecules are shown in Figure 5.

In addition to dimer structures, the structure of the cyclic HCOF dimer with a triple −H···O− hydrogen bond was optimized. Since the computational Gibbs free energy of formation of a trimer is higher than for dimers, it is energetically unlikely that trimers are formed to a significant extent.

Discussion

The infrared spectra of the HCOF monomer and the known dimers are in agreement with the previous experimental reports,[9,15] and the splitting of the monomer absorptions can be ascribed to well-known matrix site-effects. For formaldehyde,

TABLE 3: The Spectral Shifts (in cm^{-1}) of the Dimer (I−IV) Vibrations with Respect to the HCOF Monomer

		calcd (D−M)					
	expt (D−M)	I	II	III	IV	V[a]	VI[a]
CH	16.3/17.1	8.4/26.0	20.3	13.1/24.7	18.8	10.0/21.8	14.3/23.5
CO	−10.8 - −11.9	−3.0/−7.5	−8.3	−9.2/1.6	−1.9	−10.4/−4.0	−6.1/−0.5
HCF	Vw	1.6/12.5	0.2	2.0/−5.5	1.6	−1.0/5.5	−3.7/1.3
CF	0.2/0.7	18.8/−14.1	0.5	17.8/−37.3	−20.7	5.1/16.5	−27.8/4.2
OPLA	Vw	4.6/14.0	15.5	11.2/9.3	2.1	−1.1/12.3	0.8/8.0
FCO	7.7/7.9	5.3/−2.3	7.4	−7.5/6.3	7.5	3.5/7.6	−4.8/4.9

[a] BSSE uncorrected data.

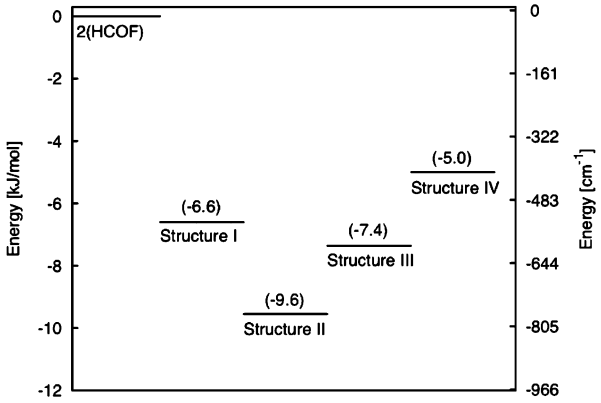

Figure 5. The computed dimerization energies of the HCOF dimers. The level of theory is MP2(FULL)/6-311++G** including the BSSE correction. The energies are corrected for zero-point energies. The values in parentheses are in kJ/mol units.

similar site splitting has been observed for all fundamentals except the ν_5 mode in the nitrogen matrix, but interestingly no splitting is observed in the argon matrix.[22−24] Examples of other small polyatomic molecules showing distinct site splitting include, for example, *cis*- and *trans*-formic acid in argon matrix and HONO in krypton matrix.[25,26] Typically, the relative intensity of the doublets is sensitive to deposition temperature and annealing of the matrix. On the basis of these observations and the existing literature we suggest that the doublets belong to HCOF monomers trapped in different matrix sites.

The red-shifted shoulder bands of the monomer absorptions most probably belong to some thermally unstable species, for example two nearby HCOF molecules or HCOF interacting with another molecule. During annealing of the matrix, the shoulder absorptions bleached completely, the dimer absorptions gained intensity, and new absorptions appeared or gained intensities. Since the monomer absorptions sharpened and slightly lost their intensity, the shoulder bands most probably do not belong to monomers trapped in different sites. Instead, the increase of the dimer absorptions at 1818 and 672 cm^{-1} during annealing would suggest that the disappearance of the shoulder bands contributes to formation of stable dimer structures. Upon being annealed, some peaks, other than the dimer peaks, increased their intensity as well. These absorptions grew even more strong when carbon monoxide was added to the HCOF/Ar mixture (see Figure 2). This observation can be taken as evidence that some amount of carbon dioxide forms complexes with HCOF. According to these observations we suggest that the red-shifted shoulder bands of the HCOF monomer and CO belong to thermally unstable structures of the HCOF dimer and the HCOF···CO complex.

Deposition at elevated temperature, 25 K for argon and 30 K for krypton, yielded a number of absorptions near the monomer lines. Interestingly, a new absorption appeared at 3013 and 3006.6 cm^{-1} in argon and krypton, respectively, and is ca. 17 cm^{-1} blue shifted from the CH-stretching fundamental. When the HCOF/Ar or HCOF/Kr ratio was varied, these absorptions showed relative changes in their intensities, which correlated with changes in the known red-shifted dimer bands associated with other vibrational modes. On the basis of these observations we assign the weak 3013 and 3006.6 cm^{-1} absorptions to the HCOF dimer in argon and krypton matrix, respectively.

To support spectral assignment we employed MP2(FULL)/6-311++G** calculations for the HCOF monomer and the dimer structures and harmonic frequencies. The computed properties of the monomer and dimers are in agreement with the former ab initio[8,27,28,] and DFT[29,30] calculations. The C−H bond is shortened by 0.0005−0.0014 Å and harmonic C−H stretching vibrations are blue shifted in dimers with respect to the monomer (Table 1). The spectral shifts of selected vibrational modes of the dimers are collected in Table 3.

The contacting −H···O− and −H···F− hydrogen bond lengths obtained in the present study (with all electrons correlated and including BSSE correction at every iteration step) are typically ∼0.06 and ∼0.12 Å, respectively, longer than those reported in ref 8. This elongation of the hydrogen bond is suggested to originate from the incapability of the basis set to describe the dispersion interaction correctly as demonstrated for a planar formaldehyde dimer with a double −H···O− hydrogen bond.[8] For comparison, we optimized this structure by including the BSSE correction and observed a 0.07 Å elongation of the hydrogen bond length compared to the BSSE uncorrected structure, and 0.16 Å elongation if compared to the MP2/aug-cc-pVQZ optimized structure.[8]

The dimerization energies of structures I and IV are nearly identical without the BSSE correction, while the BSSE correction destabilizes structure IV possessing double −H···F− hydrogen bonds. For this structure, the BSSE corrected dimerization energy is 60% of the uncorrected energy; moreover, the hydrogen bond lengths are relatively sensitive to the BSSE correction. Since the dimerization energies are corrected for BSSE, while the basis set underestimates dispersion interaction, only four stable dimer structures are found in the present study. This is a methodology problem, and it should be noted when studying weakly bound systems.

The spectral shifts of the vibrational frequencies of HCOF dimers with respect to monomer frequency are shown in Figure 6. Comparison of the computed IR intensities and experimental spectrum would suggest that structures I, III, and IV may not be abundant in our samples. This is consistent with the energy level diagram of Figure 5. Consequently, the most stable structure II is the obvious candidate for the origin of the experimentally observed dimer spectrum. At this point we recall that it was suggested in ref 8 that molecular properties are more consistent if calculated without the BSSE correction. This may be fortuitous and caused by the inadequate basis set. Nevertheless, we cannot explicitly exclude structures V and VI without examining the system with more extensive basis sets.

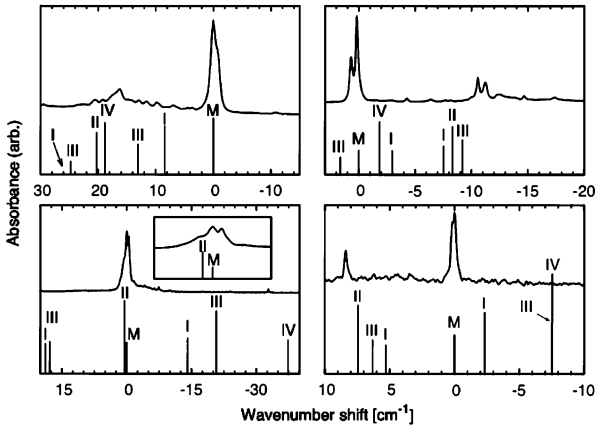

Figure 6. Experimental and computed (MP2/6-311++G** with BSSE correction) vibration spectra of HCOF (M) and structures I−IV of $(HCOF)_2$: upper left panel, CH-stretch ($M = 2996.7$ cm^{-1}); upper right, CO-stretch ($M = 1829.4$ cm^{-1}); lower left, CF-stretch ($M = 1056.5$ cm^{-1}); lower right, FCO-bend ($M = 664.4$ cm^{-1}). The *x* axes correspond to relative shifts from the monomer line. The computed spectra are shifted to match the experimental monomer lines.

To provide more detailed analysis of the IR spectrum of HCOF complexes, the geometries and the harmonic frequencies of the complexes, including HCOF···CO complexes and higher HCOF aggregates, need to be studied in detail with adequate methods.

Conclusions

Infrared spectroscopy of HCOF dimers was investigated in argon and krypton matrixes. Deposition of gas mixtures with relatively high HCOF content at elevated temperatures was observed to favor formation of dimers. Interestingly, at high dimer concentration new absorption lines were observed on the blue side of the C−H stretching fundamental of the HCOF monomer. Experimental observations indicate that the absorption, ∼17 cm^{-1} blue shifted from the HCOF monomer, possesses behavior equal to the known dimer absorptions, when experimental conditions were varied. According to these observations we suggest that the blue-shifted absorptions at 3013 and 3007 cm^{-1} belong to the HCOF dimer in argon and krypton matrixes, respectively.

Quantum-chemical calculations provide additional support to the experiment. The most stable dimer structure has two C−H··O hydrogen bonds, and the calculation of the harmonic frequency predicts a blue shift of ca. 20 cm^{-1} of the C−H stretching frequency with respect to the monomer. According to these observations, the HCOF dimer can be added to the list of experimentally studied hydrogen bonded C−H··O systems, where the formation of hydrogen bond induces a blue shift of the C−H stretching frequency.

References and Notes

(1) Jefferey, G. A. *An Introduction to Hydrogen Bonding*; Oxford University Press: New York, 1997.
(2) Scheiner, S. *Annu. Rev. Phys. Chem.* **1994**, *45*, 23 and references therein.
(3) Budesinsky, M.; Fiedler, P.; Arnold, Z. *Synthesis* **1989**, 858.
(4) Hobza, P.; Havlas, Z. *Chem. Rev.* **2000**, *100*, 4253.
(5) Hobza, P.; Havlas, Z. *Theor. Chem. Acc.* **2002**, *108*, 325.
(6) Barnes, A. J. *J. Mol. Struct.* **2004**, *704*, 3.
(7) Zierkiewicz, W.; Jurecka, P.; Hobza, P. *ChemPhysChem* **2005**, *6*, 609.
(8) Kovács, A.; Szabó, A.; Nemcsok, D.; Hargittai, I. *J. Phys. Chem. A* **2002**, *106*, 5671.
(9) Ahokas, J. M. E.; Vaskonen, K. J.; Kunttu, H. M. *J. Phys. Chem.*, in press.
(10) Olah, G. A.; Kuhn, S. J. *J. Am. Chem. Soc.* **1960**, *82*, 2380.
(11) Møller, C.; Plesset, M. S. *Phys. Rev.* **1934**, *46*, 618.
(12) Frisch, M. J.; Trucks, G. W.; Schlegel, H. B.; Scuseria, G. E.; Robb, M. A.; Cheeseman, J. R.; Montgomery, J. A., Jr.; Vreven, T.; Kudin, K. N.; Burant, J. C.; Millam, J. M.; Iyengar, S. S.; Tomasi, J.; Barone, V.; Mennucci, B.; Cossi, M.; Scalmani, G.; Rega, N.; Petersson, G. A.; Nakatsuji, H.; Hada, M.; Ehara, M.; Toyota, K.; Fukuda, R.; Hasegawa, J.; Ishida, M.; Nakajima, T.; Honda, Y.; Kitao, O.; Nakai, H.; Klene, M.; Li, X.; Knox, J. E.; Hratchian, H. P.; Cross, J. B.; Bakken, V.; Adamo, C.; Jaramillo, J.; Gomperts, R.; Stratmann, R. E.; Yazyev, O.; Austin, A. J.; Cammi, R.; Pomelli, C.; Ochterski, J. W.; Ayala, P. Y.; Morokuma, K.; Voth, G. A.; Salvador, P.; Dannenberg, J. J.; Zakrzewski, V. G.; Dapprich, S.; Daniels, A. D.; Strain, M. C.; Farkas, O.; Malick, D. K.; Rabuck, A. D.; Raghavachari, K.; Foresman, J. B.; Ortiz, J. V.; Cui, Q.; Baboul, A. G.; Clifford, S.; Cioslowski, J.; Stefanov, B. B.; Liu, G.; Liashenko, A.; Piskorz, P.; Komaromi, I.; Martin, R. L.; Fox, D. J.; Keith, T.; Al-Laham, M. A.; Peng, C. Y.; Nanayakkara, A.; Challacombe, M.; Gill, P. M. W.; Johnson, B.; Chen, W.; Wong, M. W.; Gonzalez, C.; Pople, J. A. *Gaussian 03*, revision B.02; Gaussian, Inc.: Wallingford, CT, 2004.
(13) Krishnan, R.; Binkley, J. S.; Seeger, R.; Pople, J. A. *J. Chem. Phys.* **1980**, *72*, 650.
(14) Boys, S. F.; Bernardi, F. *Mol. Phys.* **1970**, *19*, 553; Simon, S.; Duran, M., Dannenberg, J. J. *J. Chem. Phys.* **1996**, *105*, 11024.
(15) Shatte, G.; Willner, H.; Hoge, D.; Knözinger, E.; Schrems, O. *J. Phys. Chem.* **1989**, *93*, 6025.
(16) Jacox, M. E. *Chem. Phys.* **1994**, *189*, 149.
(17) Margulès, L.; Demaison, J.; Boggs, J. E. *J. Phys. Chem. A* **1999**, *103*, 7632.
(18) Ford, T. A.; Glasser, L. *J. Mol. Struct.: THEOCHEM* **1997**, *398*−*399*, 381.
(19) Qian, W.; Krimm, S. *J. Phys. Chem. A* **2002**, *106*, 11663.
(20) Hermida-Ramón, J. M.; Ríos, M. A. *Chem. Phys. Lett.* **1998**, *290*, 431.
(21) Miller, R. F.; Curl, R. F., Jr. *J. Chem. Phys.* **1961**, *34*, 1847.
(22) Nelander, B. *J. Chem. Phys.* **1980**, *73*, 1026.
(23) Nelander, B. *J. Chem. Phys.* **1980**, *72*, 77.
(24) Vaskonen, K. J.; Kunttu, H. M. *J. Phys. Chem. A* **2003**, *107*, 5881.
(25) Maçôas, E. M. S.; Lundell, J.; Pettersson, M.; Khriachtchev, L.; Fausto, R.; Räsänen, M. *J. Mol. Spectrosc.* **2003**, *219*, 70.
(26) Khriachtchev, L.; Lundell, J.; Isoniemi, E.; Räsänen, M. *J. Chem. Phys.* **2000**, *113*, 4265.
(27) Goddard, J. D.; Schaefer, H. F., III. *J. Chem. Phys.* **1990**, *93*, 4907.
(28) Fang, W.-H.; Liu, R.-Z. *J. Chem. Phys.* **2001**, *115*, 5411.
(29) Zhou, Z. Y.; Cheng, X. L.; Fu, H.; Zhou, X. M. *Struct. Chem.* **2004**, *15*, 185.
(30) Jalbout, A. F.; El-Nahas, A. M. *J. Mol. Struct.: THEOCHEM* **2004**, *671*, 125.